

# The structure of solvent crazes in polystyrene

HEIDER G. KRENZ, EDWARD J. KRAMER, DIETER G. AST

*The Department of Materials Science and Engineering and the Materials Science Center, Cornell University, Ithaca, New York, USA*

The structure of crazes grown in polystyrene (PS) immersed in *n*-heptane and methanol at room temperature has been determined using refractive index measurements, transmission electron microscopy, and fractographic analysis of craze fracture surfaces. *n*-heptane crazes in thin films exhibit a low number density of thick, load-bearing fibrils whereas methanol crazes consist of a highly interconnected network of fibrils not unlike the craze structure found in crazes grown in air. A row of large voids at the centre line of the craze which is typical of the structure observed in air crazes is not found, however, in either methanol or *n*-heptane crazes, indicating a different growth mechanism for the solvent crazes. The craze structure found in thin films is in agreement with the void contents determined from refractive index measurements and with the results from scanning electron microscopy of fracture surfaces of bulk crazes grown with methanol and *n*-heptane. Glass transition temperature measurements of equilibrium swollen PS films give  $T_g = 91^\circ\text{C}$  for methanol and  $T_g = 6^\circ\text{C}$  for *n*-heptane. The results suggest that the structure of crazes grown with slowly diffusing crazing agents (methanol and *n*-heptane) is strongly dependent on whether the growth temperature is above or below  $T_g$ , the glass transition temperature of the plasticized region just ahead of, and in, the craze. If  $T_g$  is below the growth temperature, weak crazes are formed with a large void content. During the growth, thin fibrils break by viscous flow leaving only a small number of load-bearing fibrils. The stress in the neighbourhood of the growing craze is strongly relieved favouring propagation of a single craze. If  $T_g$  is above the growth temperature, strong crazes are formed with the fibrils strain-hardened during the growth process. There is hardly any change in stress next to the craze and therefore multiple crazing (craze bundles) is favoured over the propagation of a single craze.

## 1. Introduction

In the preceding paper [1] we have demonstrated that the mechanical properties of methanol and *n*-heptane crazes in polystyrene (PS) are very different, the methanol crazes being strong and load-bearing whereas the *n*-heptane crazes are weak and easily converted into cracks. It is logical to seek the origin of these differences in mechanical behaviour in the structure of the two types of solvent crazes. In this paper we show that indeed the structure of a methanol craze in PS is radically different from that of an *n*-heptane craze. We believe the differences can be traced to the

different degree of plasticization of the craze matter by the two liquids. In this paper the first section reports the results of refractive index measurements on the two types of crazes, the second section contains measurements of the glass transition temperature  $T_g$  of equilibrium swollen PS film, the third section is an account of our direct transmission electron microscopy observations of the solvent crazes in thin films, the fourth section gives the details of the craze structure that can be inferred from microscopic observations of the fracture surfaces. The final section is a discussion in which a general model for

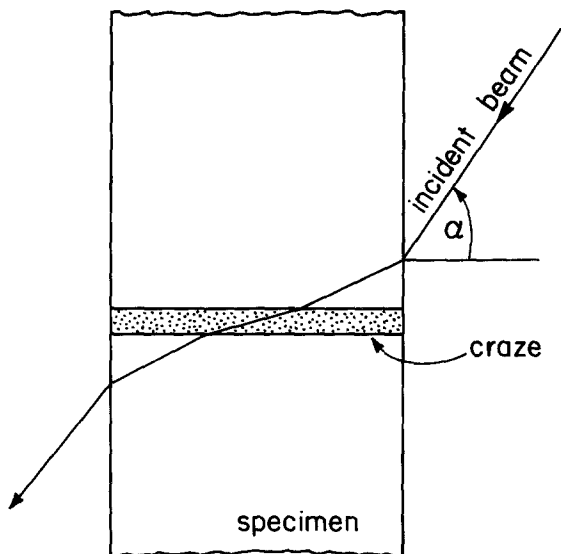


Figure 1 Schematic diagram of the optical method for measuring the refractive index of crazes. Craze thickness is magnified.

the development of solvent craze structure and mechanical properties is outlined to account for our results.

## 2. Refractive index measurements

Rectangular strip specimens (160 mm  $\times$  15 mm  $\times$  1.1 mm) were cut from commercial polystyrene (PS) sheet ( $\bar{M}_w = 314 \times 10^3$ ,  $\bar{M}_n = 97.8 \times 10^3$ ) and precracked midway at one edge. A craze was grown from that precrack using methanol or *n*-heptane as the crazing agent. Details of the precracking and crazing process are given in [1]. The refractive index of the craze was measured using a method developed by Kambour [2] and shown schematically by the ray diagram in Fig. 1. The specimen surface was polished prior to crazing to remove as much light scattering due to surface roughness as possible. The beam of a Ar-ion laser was expanded and collimated to a beam of 1 cm diameter. The specimen could be rotated in the beam about the long axis of the crack and craze. The angle  $\alpha$  between the perpendicular to the specimen surface was measured with a protractor while the image of the craze was observed on a screen behind the specimen. At small angles,  $\alpha$ , the light hitting the craze undergoes total internal reflection and the craze appears dark on the screen. At a critical angle,  $\alpha_c$ , the craze becomes transparent. Using Snell's law, the refractive index of the craze,  $n_{\text{craze}}$ , can be calculated to be:

$$n_{\text{craze}} = n_{\text{PS}} \cos \left[ \arcsin \left( \frac{\sin \alpha_c}{n_{\text{PS}}} \right) \right], \quad (1)$$

where  $n_{\text{PS}}$ , the refractive index of PS, is 1.6. The density of the craze  $\rho_{\text{craze}}$  is related to its refractive index by the Lorentz-Lorenz relation [3]:

$$\rho_{\text{craze}} = \frac{n_c^2 - 1}{n_c^2 + 2} \frac{1}{p} \quad (2)$$

where  $p$  is the specific refraction of the polymer ( $p_{\text{PS}} = 0.325 \text{ [cm}^3 \text{ g}^{-1}\text{]}$ ). The void content of the craze can then be computed from the difference between the bulk polymer densities and the craze density. The system has been checked using two methods. Cracks in the specimens were filled with a liquid whose refractive index is known exactly. We chose an immersion oil commonly used for light microscopy ( $n = 1.515$ ). The refractive index of the oil-filled crack as determined from  $\alpha_c$  measurements was  $n = 1.52$ . In another experiment crazes were grown in polycarbonate (PC) with ethanol as the crazing agent. As Kambour has pointed out, this system is particularly suitable for total internal reflection measurements, because usually thick, single crazes can be obtained. Kambour determined the void content of these crazes to be 45% [4]. Our measurements gave a void content of 49%. To measure low craze refractive indices Kambour attached glass prisms across the craze to couple the light beam into the specimen. However, we found in our experiments that some of the silicone grease, which was used to attach the glass prisms to the polymer surface, was pressed into the craze, leading to erroneous results. Therefore, we used no coupling prisms which meant that the high refractive index of the polymer limited the measurements of the craze refractive index. The lowest refractive index that could be measured was  $n_c = 1.25$  corresponding to a void content of 55.4%. The limit on  $n_c$  made direct measurements of the craze grown under *n*-heptane impossible, because its refractive index is very low. Therefore, different *n*-heptane crazes dried under strain, were filled with immersion oil ( $n = 1.515$ ) or *n*-heptane ( $n = 1.385$ ). Calculations of the refractive index from  $\alpha_c$  measurements yielded  $n_c = 1.505$  and  $n_c = 1.385$ , respectively. Within the accuracy of the experiment we can conclude that the void content of dry *n*-heptane crazes must be close to 100%. They are, nevertheless, true crazes, because upon increasing the strain they fractured with an audible signal. Crazes

grown under methanol were dried out and tested under strain. The refractive index of these crazes was  $n_c = 1.39$ , compared with the refractive index of the bulk,  $n_{PS} = 1.6$ . The void content of the methanol crazes was  $30\% \pm 10\%$ .

### 3. Glass transition temperature measurements of swollen PS

Thin films of PS were cast from a PS-benzene solution and these films were then annealed below  $T_g$  for 24 h in vacuum. Since the standard method for measuring the glass transition temperature  $T_g$  of polymers is differential scanning calorimetry (DSC), the  $T_g$  of these films was measured using DSC. At  $T = 102^\circ\text{C}$  we found the characteristic step in the DSC trace that indicates the glass transition. Other pieces of the film were swollen with *n*-heptane or methanol. No reproducible glass transition temperatures could be determined for these films by DSC methods although an indication of a transition at  $\sim 90^\circ\text{C}$  in methanol soaked films was usually present. The use of hermetically sealed cups and careful removal of excess solvent from the films did not improve the measurements. Even at temperatures well below the boiling point of the solvent random oscillations occur in the DSC trace. Similar difficulties in measuring the glass transition temperature of swollen polymers with DSC methods are also reported elsewhere in the literature [5, 6].

Therefore, we measured the  $T_g$  of swollen films by a different method, taking advantage of the abrupt drop of the elastic modulus above the glass transition temperature. Films, approximately  $1\ \mu\text{m}$  thick, were soaked at room temperature in *n*-heptane or methanol until equilibrium was reached. The time required to reach equilibrium was calculated using the diffusion coefficients of *n*-heptane and methanol in PS. The initial diffusion coefficients (at low solvent concentrations) were  $4 \times 10^{-14}$  and  $2 \times 10^{-12}\ \text{cm}^2\ \text{sec}^{-1}$ , respectively, and were determined by weight gain measurements using a microbalance [7]. Because of the extremely slow diffusion of *n*-heptane and methanol in PS, thin films must be used to keep the time for complete penetration of the crazing agent to reasonable levels. A disadvantage is that these thin films are extremely hard to handle, making experiments with them difficult.

To determine the  $T_g$  of the *n*-heptane swollen films, one end of the film, a  $3\ \text{mm} \times 10\ \text{mm}$  rectangular strip, was wedged between two metal

blocks. The film was stiff enough for the other end to protrude as a cantilever beam. The blocks were located in a Petri dish which was filled with *n*-heptane. After some time the cantilever end of the film became limp and sagged so that it almost made a right-angle bend after emerging from the blocks. The drop of modulus indicated that  $T_g$  of the *n*-heptane swollen film was below room temperature. The dish was then cooled and the temperature of the metal blocks was measured with a thermocouple. At  $-100^\circ\text{C}$  the now glassy film was turned between the blocks such that it formed a right angle pointing upwards. The dish was then allowed to warm up in air. The onset of the first noticeable sagging of the protruding end of the film was taken to be the glass transition temperature. We found  $T_g$  to equal  $6^\circ\text{C}$ .

Soaking films in methanol does not produce a softening of the films, indicating that  $T_g$  of these films is above room temperature. Because the boiling point of the methanol is  $65^\circ\text{C}$ , and the  $T_g$  is expected to be higher after equilibrium soaking, the films were removed from the methanol for the experiment. One end of the film was again wedged between two blocks and the assembly was placed on a hot plate. The temperature of the blocks close to the polymer film was recorded. The temperature was increased by  $15^\circ\text{C}\ \text{min}^{-1}$ . The first sagging of the free end of the film was observed at  $91^\circ\text{C}$ . This value for methanol swollen PS is in agreement with the result of Kambour *et al.* ( $T_g = 90^\circ\text{C}$ ) [6]. Our value for *n*-heptane swollen PS of  $T_g = 6^\circ\text{C}$  is higher than their (DSC) value ( $T_g = -11^\circ\text{C}$ ), but considering the difficulties in interpreting the DSC traces they are in reasonable agreement.

As a final check on our system, a dry PS film was placed between the blocks on the hot plate and heated up. We found  $T_g$  equal to  $101^\circ\text{C}$  which is in good agreement with the  $T_g$  we obtained from DSC experiments.

## 4. Transmission electron microscopy of crazes in PS films

### 4.1 Experimental procedure

In order to investigate solvent crazes in the films of PS with the transmission electron microscope, the films have to be strained, crazed with a crazing agent, and then inserted into the microscope without relaxing the overall strain. Straining of thin films of PS is very difficult. The films are extremely notch sensitive and any inclusion or pore

due to the casting or any notch due to cutting the specimen will produce failure of the specimen at very small strains.

We avoided these problems by using a new technique. A coarse copper grid (2 lines/mm) was cut into rectangular strips (5 mm × 50 mm) which were annealed for 1 h at 600°C under vacuum such that they could be easily plastically deformed. The strips were dipped into a solution of 2.5% PS in benzene, dried in air, and subsequently annealed for 12 h under vacuum at 100°C. Owing to its surface tension, the polymer contracted and coated the copper wires, leaving the spaces between the wires free of polymer. Meanwhile, PS films, approximately 10 μm thick, were cast from more dilute solutions (0.5% PS in benzene) on pieces of rocksalt. These films were also annealed in vacuum at 100°C for 12 h to remove the solvent. They were then floated off the rocksalt substrate in a waterbath and deposited onto the coated copper grid strips. The copper grid with the PS coating and the film on it was then annealed in vacuum at 102°C, the glass transition temperature of PS, for 15 min. This treatment caused the films to adhere to the PS coating of the wires. The film can now be easily strained by straining the copper strip in a small tensile stage, but developing cracks propagate only one grid square and do not destroy the specimen. The plastic deformation of the copper grid enforces and supports the predominantly elastic deformation of the dry PS films even if the grid is taken out of the strain frame. Another advantage of the technique is that electron microscope specimens can be directly punched out of the copper grid without unloading the polymer film.

The specimens were directly inserted into the transmission electron microscope (JEM 200) and checked to see if dry crazing had occurred during the straining process. The films were inspected at 200 keV and low magnification was normally used to keep radiation damage at a minimum. After the first inspection the specimen was taken out of the microscope, but left in the specimen holder, which was then immersed in a crazing agent, *n*-heptane or methanol. After a few minutes the specimen was dried in air and again inserted in the microscope. Usually it is possible to find again cracks or holes in the film which did not initiate air crazes (were craze-free) during the first inspection. These cracks and holes cause stress concentrations in the film usually sufficient to initiate solvent crazes.

## 4.2. Craze structure

Fig. 2a shows portions of a craze grown with *n*-heptane as a crazing agent. Fig. 2b, c and d are higher magnifications of selected regions of the craze. The very few connecting fibrils correlate very well with the mechanical weakness of *n*-heptane crazes observed previously [1]. The average thickness of the fibrils as measured along the middle of the craze is 2500 Å. The void content of the craze, determined by weighing the different fibril and void portions cut out of a photograph of the craze [8], is 70%. This number appears to be too low when compared with the measurements of strength and refractive index, but it only represents the projected void area fraction. It does not take into account the contraction of the fibrils in the direction of the film thickness. This lateral contraction is quite large, because the electron beam penetrates the fibrils very well, but not the film. Assuming cylindrical fibrils, a rough estimate of the void content, based on the original 10 μm film thickness, is 99.25%.

At several spots, particularly at the craze base, fibrils break during the crazing process, i.e. in the presence of *n*-heptane. The broken fibrils form bundle-like structures as shown with arrows in Fig. 2b. In other spots load-bearing fibrils break in the electron beam (arrow B) as a comparison of Fig. 2a and c shows. These fibrils have been broken in the absence of *n*-heptane. They are stiff and stand by themselves rather than forming bundles with other fibrils. This difference between *n*-heptane craze failure in the dry and in the wet state will be of importance in the interpretation of the fracture surfaces of bulk crazes.

*n*-heptane crazes exhibit some tie fibrils that connect the major load-bearing fibrils, a structure similar to that of air crazes in PS [9]. These tie fibrils seem to be the relics of cobweb-like films that connected the major fibrils. Following the craze from its tip to its base (Fig. 2a) one can see that the load-bearing fibrils are first connected with films which thin out and are punctured more and more as the craze thickness increases. Further towards the base, the films finally form thin tie fibrils. At the base of the craze the craze opening is generally so high that no tie fibrils remain unbroken. These broken tie fibrils will contribute to the fibril bundles mentioned above.

Another important feature of the *n*-heptane craze is the absence of a midrib as described by Beahan *et al.* [9] in air crazes in PS. Our obser-

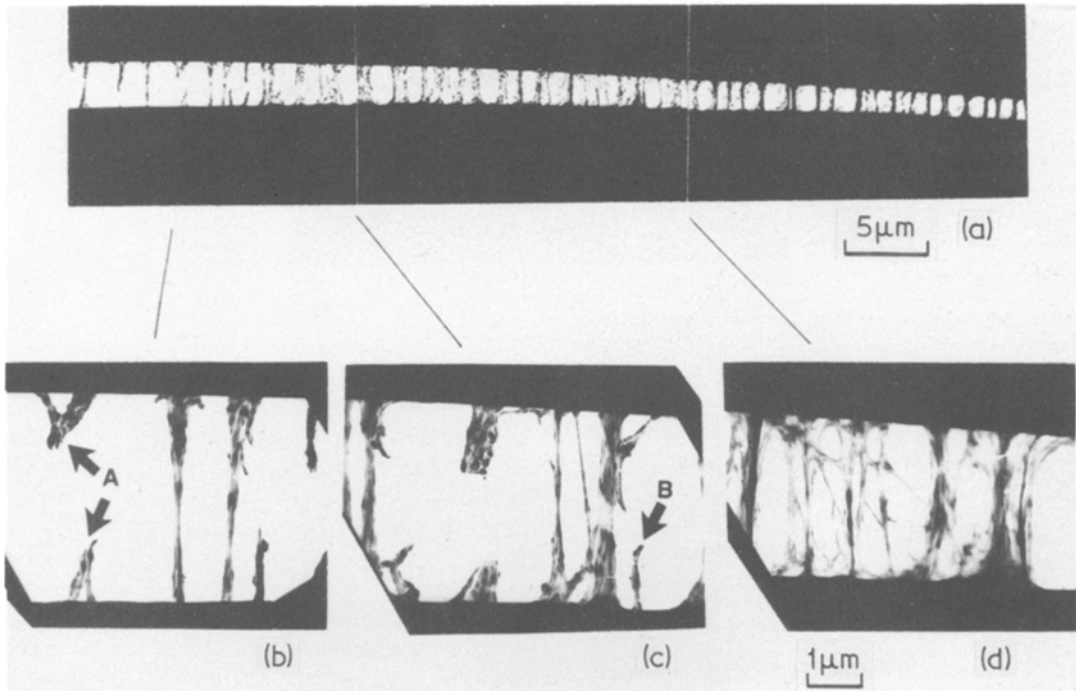


Figure 2 (a) Transmission electron micrograph of a craze grown under *n*-heptane in a polystyrene film 10  $\mu\text{m}$  thick. (b) to (d) Higher magnifications of details of (a). Arrow A in (b) shows fibrils broken in the presence of *n*-heptane. Arrows B in (c) show fibrils broken dry.

vation of air crazes confirms their finding that such crazes in PS films invariably show a midrib, i.e. a row of large voids along the centre of the craze (Fig. 3). Beahan *et al.* [9] suggest that the increase in craze thickness is mainly achieved by adding more voids to either side of the midrib. The absence of a midrib in the *n*-heptane crazes

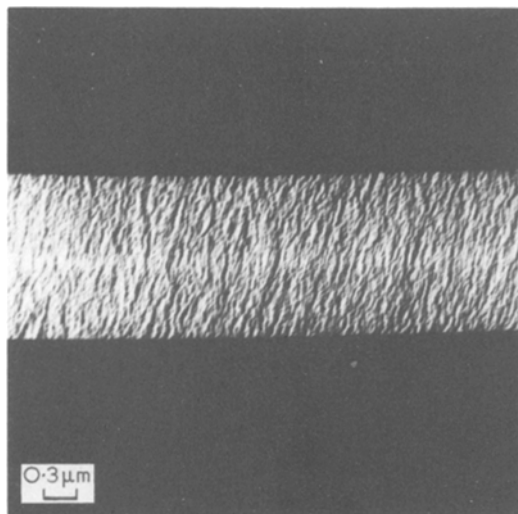


Figure 3 Transmission electron micrograph of a craze grown in air in a polystyrene film 10  $\mu\text{m}$  thick.

suggests that the thickening mechanism of these crazes must be fundamentally different from that of an air craze.

Using the same methods as for *n*-heptane crazes, we have observed the structure of methanol crazes in PS films. Fig. 4a shows a micrograph of a section of a methanol craze in a 10  $\mu\text{m}$  thick film. Fig. 4b is a higher magnification micrograph of a midportion of Fig. 4a. The craze is made up of an interconnected dense network of very fine fibrils which occasionally form fibril clusters. The individual fibre diameter of this dense network is difficult to determine accurately, but is approximately 200  $\text{\AA}$ . The fibrillar structure between the clusters does not change along the length of the craze, but the number of clusters increases towards the craze tip. Again a well-defined midrib section is not observed, although the fibrils between the clusters show almost the same interwoven structure as found in air crazes in PS.

## 5. Fractography of methanol and *n*-heptane crazes

### 5.1. Methanol crazes

Crazes were grown under tension in 1 mm thick rectangular specimens with methanol as a crazing

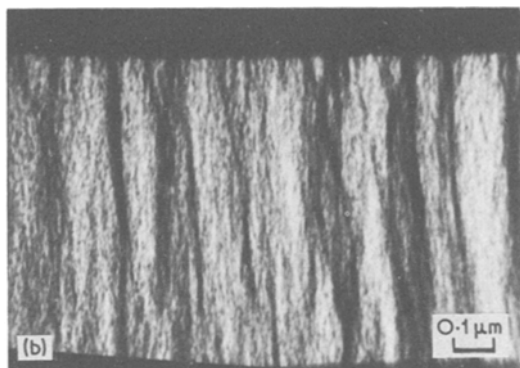
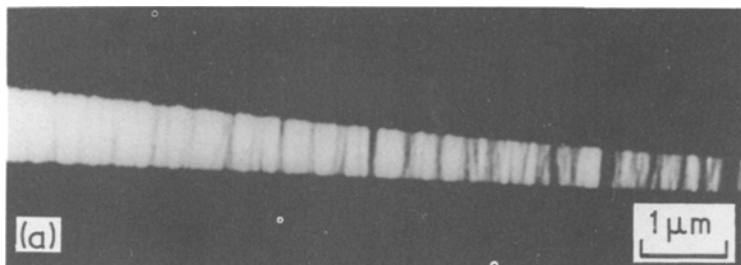


Figure 4 (a) Transmission electron micrograph of a craze grown under methanol in a polystyrene film 10 μm thick. (b) Higher magnification of the craze structure of (a).

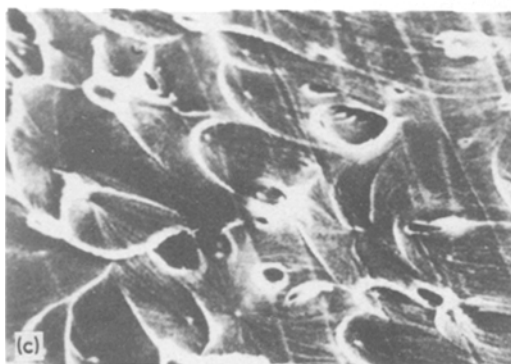
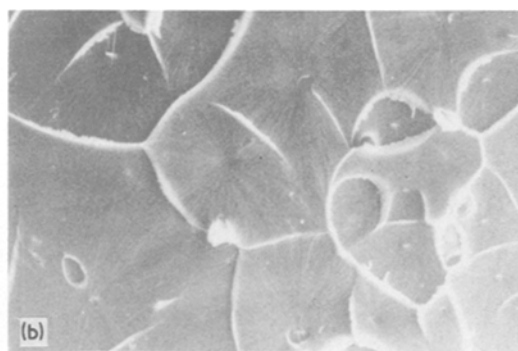


Figure 5 SEM micrographs of the fracture surface of a dry methanol craze in polystyrene; crack propagation is from (a) to (d).

agent, and were allowed to dry under strain. The strain was then increased to fracture the specimen and the fracture surfaces were coated with a thin film of gold–palladium. The fracture surfaces were then ready for investigation in the scanning electron microscope (SEM).

In view of the similarity in strength and structure between methanol and air crazes it is not surprising to find many of the features of fracture surfaces of air crazes again in the fractographs of methanol crazes. Basically an area of slow crack growth and slow parting of the craze (Fig. 5a) is followed by a transition area (Fig. 5b) where the crack speed slowly increases. In the latter region secondary fracture sites develop and combine, advancing with the main crack front by shearing off ridges that separate the smaller regions of secondary fracture. The overall crack speed is still slow, as is demonstrated by the almost circular ridges around the secondary fracture events. Owing to the slow crack growth bundles of fibrils are found radially oriented around the nucleation sites of the secondary fracture events leaving a surface texture that reminds one of brush marks radiating from these sites. As the crack speed increases, the circles around secondary fractures change shape and become ellipses and finally hyperbolae (Fig. 5c). The brush mark structure becomes more and more oriented in the direction of the crack propagation. Increasing crack speed and jumping of the crack front leads finally to an extremely rumpled, patch-like surface (Fig. 5d).

Brush mark structure and secondary fracture sites are still recognizable, but are very much smeared out. This type of surface occurs at the methanol craze tip and is almost indistinguishable from fracture surfaces produced by fast crack propagation through air crazes.

## 5.2. *n*-heptane crazes

The strong plasticization of PS by *n*-heptane and the high void content in the *n*-heptane craze leads to some complications in the interpretation of the fracture surface of these crazes. Fig. 6 shows a SEM micrograph of the fracture surface of a *n*-heptane craze that has been dried under strain and subsequently fractured by increasing the stress. It exhibits a honeycomb structure which has an average cell diameter of approximately  $1\ \mu\text{m}$  at the craze base and which becomes finer and finer towards the tip.

If, on the other hand, the craze is broken in the wet state with *n*-heptane still present, the fracture surface has a granular appearance (Fig. 7). Again the structure is coarse at the craze base and becomes finer towards its tip. Examination of the matching fracture surface shows in both cases the same morphology indicating that the craze did not break by stripping away the craze matter from the matrix–craze interface. The morphology in both cases does not agree with the expected small number density of large broken fibrils based on the observed structure of the craze in the thin films and with the void content calculated from the refrac-

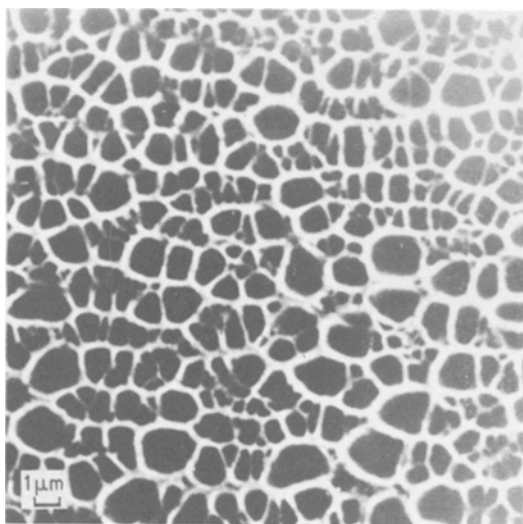


Figure 6 SEM micrographs of the fracture surface of a dry *n*-heptane craze.

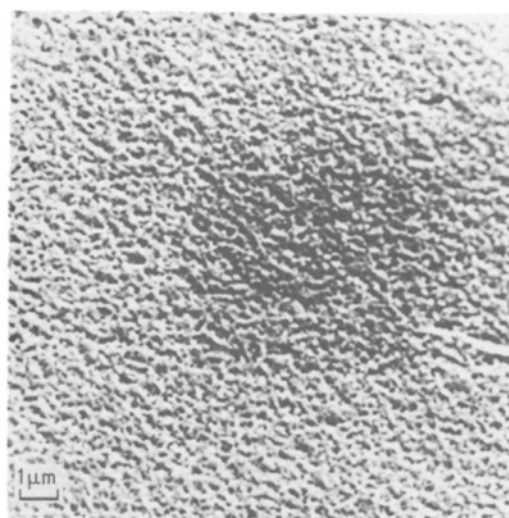


Figure 7 SEM micrograph of the fracture surface of an *n*-heptane craze broken wet.

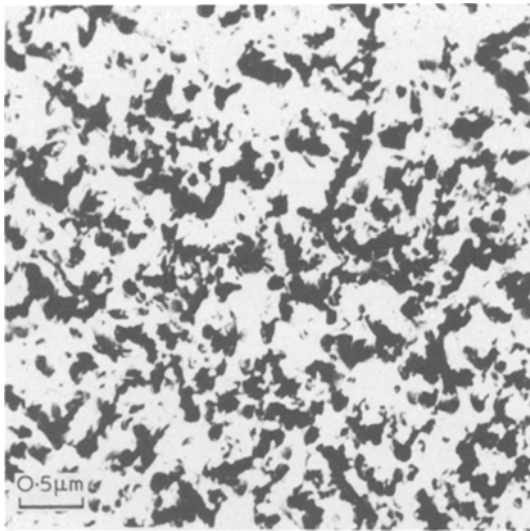


Figure 8 Polyacrylic acid replica of a fracture surface of an *n*-heptane craze broken wet.

tive index measurements. Counting the ridges of the honeycombs or the protrusions of the granular structure as load bearing fibrils would give a void content much lower than that observed.

To investigate whether the observed *n*-heptane craze fracture surface structures are dependent on specimen size or method of craze growth, *n*-heptane crazes were grown in 10 mm thick PS specimens under three-point bending. Replicas were prepared by coating the fracture surface with polyacrylic acid (PA acid). After drying the PA acid forms a thin film that can be stripped off the surface. The film was shadowed at an angle of  $10^\circ$  with gold-palladium and coated with carbon as a supporting layer. The PA acid was then dissolved

in water and the floating replica was deposited on a microscope grid for examination in the JEM 200. This method avoids the use of replicating tape which has to be dipped in acetone before it is deposited on the surface. Acetone dissolves PS quite rapidly and would certainly destroy the fracture surface. Fig. 8 shows a replica of the fracture surface of an *n*-heptane craze that has been broken wet. Again, as in the case of the craze grown in tension, the granular character of the surface with stump-like, thick fibrils is visible. Fig. 9a and b are regions of the fracture surface of the craze base and the craze tip, respectively, of an *n*-heptane craze broken dry. Fig. 9a shows again the typical honeycomb structure, but owing to the high contrast one can clearly see some isolated major fibrils that protrude out of the ridges of the combwalls. Some of them are indicated with arrows in Fig. 9a. Fig. 9b shows that close to the craze tip the polymer matter of the craze is interconnected and only very little interrupted by isolated voids, some of them are marked by arrows. The difference between the fracture surface of *n*-heptane crazes broken dry and wet could be caused by two processes. Firstly, the different nature of the fracture process in the wet versus dry condition could cause some change in morphology. Secondly, the drying process can possibly cause changes due to the surface tension forces of the liquid.

To check the first possibility *n*-heptane crazes have been dried under stress and have been broken subsequently in liquid nitrogen. Again the honeycomb structure can be detected indicating that this structure arises primarily during the drying process and is not created by the fracture process

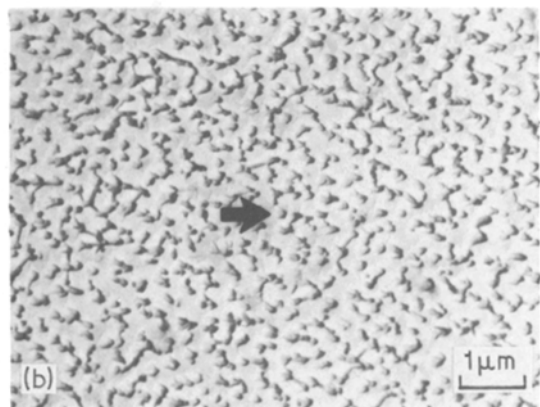
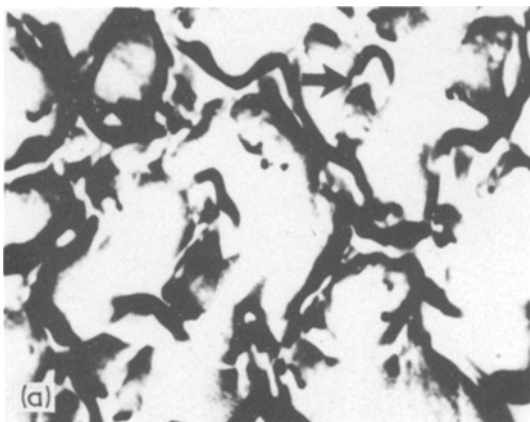


Figure 9 Polyacrylic acid replica of a fracture surface of an *n*-heptane craze broken dry: (a) craze base, arrows indicate major fibrils; (b) crack tip, arrows mark voids.



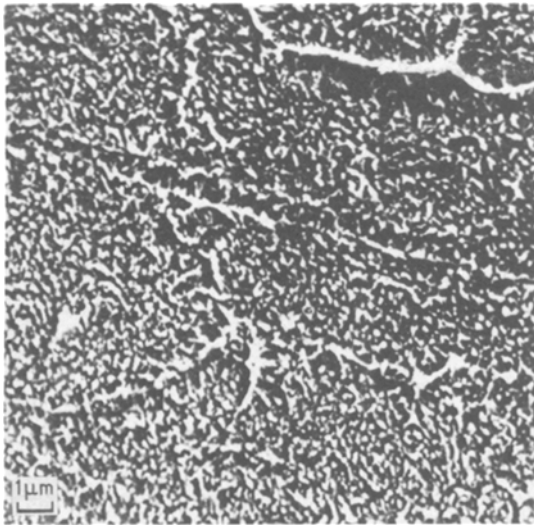


Figure 10 SEM micrograph of a fracture surface of an *n*-heptane craze broken after critical point drying.

itself. Therefore a method has to be devised to remove the *n*-heptane from the craze without the evaporation step. A critical point drying process has been used for this purpose.

While wet and under strain, isopropyl alcohol (IPA), which is miscible with *n*-heptane, was substituted for the *n*-heptane. The IPA does not craze PS at the low stress intensities used to produce *n*-heptane crazes. Ethyl alcohol (EA) in turn was substituted for IPA. (EA is miscible with IPA and liquid CO<sub>2</sub>, but not with *n*-heptane.) The specimen was placed in a pressure vessel filled with ethanol. Subsequently liquid CO<sub>2</sub> was substituted

under pressure and at room temperature for the EA. Then the pressure and the temperature were increased to the critical point of CO<sub>2</sub> (31.1° C and 74 MN m<sup>-2</sup>). At this point the liquid and the gas CO<sub>2</sub> exist without an interface and the liquid changes to gas without exerting any disturbing surface tension forces on its surroundings. The dry craze was removed from the pressure vessel, broken, and examined in the SEM. Fig. 10 shows the fracture surface. Instead of the honeycomb or the granular structure, individual fibrils can be seen.

If the honeycomb structure or the granular structure is caused by the high mobility of the plasticized fibrils then any liquid that can substitute for *n*-heptane in the craze, and which is less plasticizing should prevent the formation of these two structures and should generate a structure close to that formed by critical point drying. We therefore interrupted the critical point drying process after the substitution of IPA for *n*-heptane. The craze was then dried and broken. One half of the fractured specimen was coated with gold-palladium and examined in the SEM. The fracture surface is shown in Fig. 11a. As expected it shows nearly the same fracture surface morphology achieved by critical point drying. The matching surface was immersed for 1 h in *n*-heptane, dried and then coated. This surface is shown in Fig. 11b. The surface is smooth, no fibrils are visible. It demonstrates the total retraction of craze fibrils under the influence of *n*-heptane.

The high mobility of the plasticized fibrils can also be shown in a different way. If the *n*-heptane

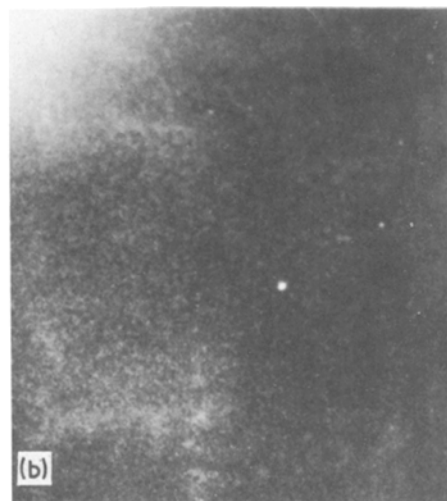
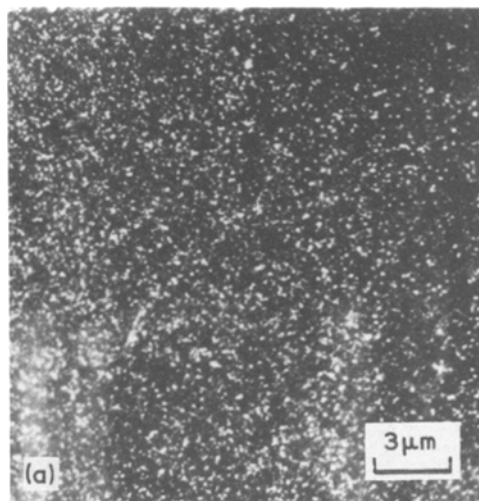


Figure 11 (a) SEM micrograph of a fracture surface of an *n*-heptane craze after the substitution of isopropyl alcohol for *n*-heptane and subsequent drying. (b) As (a) with subsequent soaking in *n*-heptane for 1 h.

craze is broken wet, one can clearly observe interference colours on the fracture surface indicating that broken fibrils are still protruding. The colours slowly fade and finally almost completely vanish.

## 6. Discussion

Based on the results of this and the preceding paper, a qualitative model can be outlined for the structure and mechanical properties of crazes grown using crazing agents which diffuse very slowly in the bulk polymer (*n*-heptane and methanol in PS are two such liquids). Generally the slowly diffusing crazing agent plasticizes only a small volume in front of the precrack or craze which then easily cavitates under applied strain and forms voids. The porous craze thus formed acts as a short-circuit diffusion path which allows plasticization of the newly exposed, unoriented, polymer at the craze tip. The void-fibril ratio and the thickness of the individual fibrils in the craze will be governed by the change in  $T_g$  that has occurred in the craze matter which is plasticized by the liquid.

If the new  $T_g$  is far above the testing temperature, as is the case for methanol in PS, the voids that form will be stable, i.e. the surrounding fibrils will not break down. Whenever the fibrils yield and form a neck they will be stabilized by strain (orientation) hardening, leading to the formation of many small voids, and many thin fibrils. This mechanism produces strong crazes. Because they are highly load bearing the tensile strain normal to the surface of the craze will be relaxed only a small amount as a result of craze growth, which has been shown experimentally in the preceding paper [1]. Therefore, this mechanism will favour craze bundles (multiple crazing), and will make it very difficult to propagate single crazes. It is virtually impossible to grow single methanol crazes in PS longer than about 1 mm [1].

If the  $T_g$  of the plasticized volume is below the testing temperature, as it is in the case of *n*-heptane crazes, the fibrillation process will be quite different. Whenever thin fibrils neck they are not stabilized by strain-hardening, but continue to neck and finally rupture by viscous flow. Small voids therefore coalesce to form large voids. Only very few thick fibrils, in which the viscous flow rate is reduced due to the lower stress, remain. The craze increases its thickness by viscous stretching of these thick fibrils. The craze will have a very high void content and will be extremely weak.

During growth of long *n*-heptane crazes, the base fibrils are exposed longer to the crazing agent and stress than those in a short craze. In a long craze, therefore, more of these fibrils will rupture, and those that remain will be thinner, and bear less load, than in a short craze. Long *n*-heptane crazes would, therefore, be weaker than short *n*-heptane crazes, which agrees with our observations of mechanical properties of these crazes in the preceding paper [1]. The stress concentration at the tip of the starter crack will be greatly reduced owing to the weakness of the propagating *n*-heptane craze (see Fig. 9 of [1]) and the largest stress concentration will occur, not at the crack tip, but at the craze tip. This redistribution of stress will favour continued propagation of a single craze over the formation of a craze bundle.

The decrease in  $T_g$  of the plasticized fibrils in the case of *n*-heptane crazes causes some difficulties in the interpretation of their fracture surfaces. If the craze is broken in the wet state, and left for a long time in the presence of *n*-heptane, all the fibrils can easily retract back into the surface (Fig. 11b). If the *n*-heptane is removed after a short time, the thicker fibrils cannot retract completely, causing a granular surface (Fig. 7). If, on the other hand, the craze is allowed to dry under stain, the evaporation of *n*-heptane will cause bubbles of gas to grow between the still load-bearing fibrils. As a bubble grows the broken and highly mobile fibrils are constrained to conform to the walls of the bubble by surface tension forces. Finally, when the bubbles impinge between the load-bearing fibrils, there will be left a ridge of broken fibril material where the walls of two bubbles met. A good estimate of the number of load-bearing fibrils is, therefore, the number of nodal points of the honeycomb structure (Fig. 6). The gathering of broken fibrils into ridges can also be observed in thin film crazes (Fig. 2, arrow A). If no surface tension forces act on the fibrils during drying, as is the case during critical point drying, or if  $T_g$  of the fibrils is increased above the testing temperature, both the retraction and the honeycomb structure is avoided. All the fibrils, originally broken and unbroken in the craze, can be seen sticking out of the fracture surface (Figs. 10 and 11).

The model outlined above must be changed if liquids are considered which can diffuse somewhat more rapidly than either *n*-heptane or methanol in PS. Instead of increased craze-opening displace-

ment occurring by increased strain of the fibrils within the craze as implicitly assumed here, additional opening displacement could result from deformation and fibrillation of the layers of un-oriented polymer at the surfaces of the craze which are also plasticized by diffusion of the crazing agent. Normally this fibrillation of unoriented material at the surface of the craze is suppressed relative to the fibrillation of material at the craze tip where the high tri-axial stress, which is smaller at the craze surfaces, enhances diffusion and absorption of the crazing liquid [10] as well as the plastic growth of voids [11]. For faster diffusing solvents or higher stresses (e.g. air crazing), however, a significant fibrillation of material at the craze surface could occur and result in a plastic strain of the craze matter that is approximately constant from the craze base to tip. Whether surface fibrillation occurs probably determines whether a distinct craze midrib (a row of larger voids inherited from the fibrillation process at the craze tip) is observed. The absence of this midrib in *n*-heptane and methanol crazes in PS is thus in agreement with the hypothesis that increases in the craze-opening displacement in these crazes occurs primarily by increasing the strain in the craze fibrils.

## 7. Conclusions

Our results indicate that the strength and structure of crazes produced by slowly diffusing solvents depend markedly on the glass transition temperature of the solvent plasticized fibrillar craze matter. If this  $T_g$  is well above the ambient temperature, the craze fibrils strain-harden, many fine load-bearing fibrils are formed and the craze is strong. If  $T_g$  is below the ambient temperature, the craze fibrils undergo viscous flow at relatively low stresses and rupture viscously at higher strains, giving rise to a craze structure which consists of very small area fraction of relatively large load-bearing fibrils. Such crazes are naturally very weak

and are easily mistaken for (and, at higher stresses, converted into) cracks. True stress-cracking agents in glassy polymers may be those liquids, with small diffusion coefficients so that crazes act as short circuit diffusion paths, which lower the  $T_g$  of the equilibrium swollen polymer well below room temperature. Whether this hypothesis will prove to be correct awaits an investigation of a wider range of liquids, polymers and craze-growth temperatures but it appears attractive based on our results to date.

## Acknowledgements

The financial support of the National Science Foundation through the Cornell Materials Science Center and the U.S. Army Research Office-Durham is gratefully acknowledged. We also appreciate useful conversations with Professor E.L. Thomas on similar methods he has devised for examining the structure of solvent crazes in thin films.

## References

1. H. G. KRENZ, E. J. KRAMER, and D. G. AST, *J. Mater. Sci.* **11** (1976)
2. R. P. KAMBOUR, *Nature* **195** (1962) 1299.
3. C. P. SMYTH, "Dielectric Behaviour and Structure" (McGraw Hill, New York, 1955).
4. R. P. KAMBOUR, *J. Polymer Sci. Part A* **2** (1964) 4159.
5. Z. VEKSLI, W. G. MILLER, and E. L. THOMAS, *J. Polymer Sci.*, to be published.
6. R. P. KAMBOUR, C. L. GRUNER, and E. E. ROMAGOSA, *J. Polymer Sci. Polymer Phys. Ed.* **11** (1973) 1890.
7. R. BUBECK, Ph.D. Thesis, Cornell University (1976).
8. E. L. THOMAS and S. J. ISRAEL, *J. Mater. Sci.* **10** (1975) 1603.
9. P. BEAHAN, M. BEVIS, and D. HULL, *Proc. Roy. Soc. Lond. A* **343** (1975) 525.
10. A. PETERLIN, *J. Macromol. Sci. - Phys.* **B11**(1) (1975) 57.
11. A. S. ARGON, *ibid* **B8** (1973) 573.

Received 30 March and accepted 3 May 1976.